Journal of Organometallic Chemistry 694 (2009) 2153–2162

Contents lists available at ScienceDirect

Journal of Organometallic Chemistry

journal homepage: www.elsevier.com/locate/jorganchem

'Click' silica immobilisation of metallo-porphyrin complexes and their application in epoxidation catalysis

Aidan R. McDonald, Nicole Franssen, Gerard P.M. van Klink, Gerard van Koten *

Chemical Biology and Organic Chemistry, Faculty of Science, Utrecht University, Padualaan 8, 3584 CH Utrecht, The Netherlands

ARTICLE INFO

Article history:
Received 3 June 2008
Received in revised form 12 February 2009
Accepted 24 February 2009
Available online 1 March 2009

Keywords:
Homogeneous catalysis
Epoxidation
Immobilisation
Click chemistry
Catalyst recycling

ABSTRACT

We present the synthesis, via Adler condensation reactions, of mono- and tetrakis-4-(ethynylphenyl)porphyrin ligands and the zinc and manganese complexes thereof. The formed complexes were immobilised on silica by reacting the ethynyl groups with azide-functionalised silica in a copper(I) catalysed Huisgens 1,3-dipolar cycloaddition reaction. The synthesised metallo-porphyrin containing materials were thoroughly characterised using various solid-state techniques (NMR, IR, UV–Vis, elemental content analysis). The manganese containing materials were applied as catalysts in the epoxidation of various alkenes (cyclooctene, cyclohexene, styrene) with various oxidants (iodosylbenzene, tert-butylperoxide). The heterogenised homogeneous catalysts show diminished activity and yields compared to the analogous homogeneous catalysts (71% yield cf. 92% for cyclooctene epoxidation, TOF 82 h^{-1} cf. 230 h^{-1}). Upon recycling, the heterogenised catalysts become gradually less active over five cycles until they are catalytically inactive. The deactivation process is discussed, with spectroscopy suggesting that the catalysts themselves are intact and thus stable to the reaction conditions and recycling, however there is likely some decomplexation, and also both chemical and mechanical decomposition of the silica support resulting in inaccessibility to the catalytic site.

1. Introduction

The immobilisation of homogeneous catalysts, and the stability of the catalyst itself, are important issues in the development of homogeneous catalytic systems for industrial application [1]. The immobilisation of homogeneous catalysts allows for ease of separation of catalyst from reactants and products, while catalyst stability is essential to recycling procedures and for the recovery of precious metal complexes. The synthesis of many of the fine chemicals essential for life and leisure involve at least one or more steps that involve the use of homogeneous catalysis [2]. The reason for this is relatively simple, selectivity. Homogeneous catalysts provide the required selectivity for certain end-products, that heterogeneous catalysts cannot offer. Thus the benefits of using heterogeneous catalysts, high stability and recyclability, are outweighed by the necessity to have selective syntheses using homogeneous catalysts. However, the cost of synthesis and recovery of homogeneous catalysts or their derivatives mean they are not widely applied. One manner to overcome this would be to immobilise homogeneous catalysts such that they can be treated in the same manner as heterogeneous catalysts, i.e. they can be recycled.

According to a recent report asymmetric epoxidation is the second most widely used asymmetric process in industry [3]. Chiral epoxides and their derivatives are extremely high value products and are the basis of many enantiopure compounds. For this reason the immobilisation of chiral epoxidation catalysts has been investigated thoroughly in recent times [4]. The field of supported metallo-porphyrins for epoxidation catalysis [5] and in particular the immobilisation of porphyrin complexes on inorganic supports and their application in alkane/alkene oxidation have been investigated [6]. What comes from these previous reports and is a general trend in the field of homogeneous catalyst immobilisation, is that *covalent* immobilisation of catalysts on *inorganic* supports is essential for good catalyst recycling results, and minimal influences on the catalytic site by the support. It is also apparent that a simple manner for the immobilisation of such homogeneous catalysts on inorganic supports is necessary. A key point to add to this is that catalyst stability should be taken into account before any attempts are made to covalently immobilise a homogeneous catalyst. Previous work has shown that highly stable coordination complexes should be used, because labile coordination complexes do not withstand the relatively harsh conditions used for catalyst immobilisation, and subsequently for the recycling of the heterogenised catalyst. The conditions for immobilisation in some systems can be detrimental to the most stable of complexes, and ideally a modular system, comprising support, linker and catalyst would be a goal, in

* Corresponding author. Fax: +31 30 252 3615.
E-mail addresses: mcdon701@umn.edu (A.R. McDonald), g.vankoten@uu.nl (G. van Koten).

0022-328X/$ - see front matter © 2009 Elsevier B.V. All rights reserved.
doi:10.1016/j.jorganchem.2009.02.020

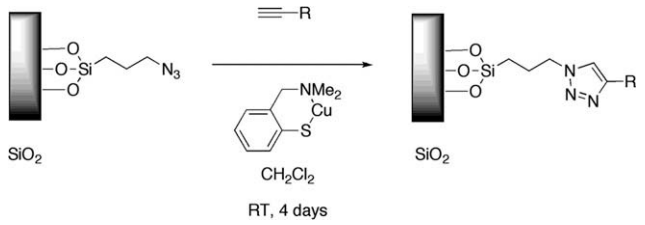

Scheme 1. Copper(I) thiolate catalysed 'Click' coupling of ethynyl organic moieties to silica support.

which mixing, under mild conditions, of the various components together resulted in the immobilised catalyst.

We have recently demonstrated such a system in which the immobilisation of homogeneous catalysts on an inorganic support is mediated using 'click' immobilisation techniques involving an azide linked to a high density silica support (Fig. 1) [7]. 'Click' immobilisation is defined by high yielding, highly atom efficient reactions for the tethering of an organic or organometallic moiety to an inorganic support. Azide-functionalised silica has been used to couple ethynyl-functionalised compounds to high density silica using a copper(I) catalysed 1,3-Huisgens dipolar cycloaddition reaction. The Huisgens dipolar cycloaddition is very prominent in organic chemistry presently, because of its high yielding, high atom efficiency and selectivity. The reaction has been classified as a 'Click' reaction, because of its high yielding, efficient nature, and its low by-product production [8] (see Scheme 1).

In this report immobilisation of manganese and zinc porphyrin complexes was mediated through the copper(I) thiolate catalysed reaction of an acetylene-functionalised porphyrin complex with the aforementioned azide-functionalised silica support. The novel materials were fully characterised using solid-state spectroscopic techniques. The synthesised manganese materials were applied as catalysts in the epoxidation of various alkenes showing results comparable to the homogeneous catalyst system. However, upon recycling the catalytic material showed considerably diminished activity. The porphyrin ligand system is acknowledged to be highly stable and rigid, however, the epoxidation reactions that metal porphyrin complexes catalyse use oxidants that can have great effects on complex stability, but also that give side reactions and we believe this is one of the sources of the deactivation of the catalytic manganese materials.

2. Results and discussion

2.1. Synthesis of silica-bound porphyrin complexes

For ethynyl-functionalised porphyrin synthesis (Scheme 2), mono-trimethylsilyl (mono-TMS) protected ethyne was coupled with 4-bromo-benzaldehyde yielding 4-[(trimethylsilyl)ethynyl]benzaldehyde (**1**) in a palladium catalysed Sonigashira coupling reaction (79% yield). Aldehyde **1** was applied in an Adler porphyrin synthesis in two manners [9]. Similar compounds have been previously synthesised [10]. Firstly, **1** was mixed in a 1:1 ratio with pyrrole in refluxing propionic acid yielding 5,10,15,20-tetrakis-(4-[(trimethylsilyl)ethynyl]phenyl)-porphyrin (**2**). Compound **2** was reacted with both manganese(II) and zinc(II) acetates to yield complexes **3** and **4**, respectively, in relatively high yields. Secondly compound **1** was reacted with pyrrole and benzaldehyde (1:6:7 molar ratio, respectively) to synthesise 5-(4-[(trimethylsilyl)ethynyl]phenyl)-10,15,20-trisphenylporphyrin (**5**).

Compound **5** could not be completely purified (TPP, with small amounts of bis-, tris- and tetrakis- substituted porphyrins were also formed in the synthetic process) and complexation with $Mn(OAc)_2$ was carried out on the mixture of functionalised ligands. Column chromatography was used to isolate the mono-ethynyl porphyrin manganese complex from the other products. However, it was not possible to separate **6** and [MnCl(TPP)] (TPP = 5,10,15,20-tetrakisphenylporphyrin). Nevertheless, for the immobilisation of **6** on silica, the **6**/[MnCl(TPP)] mixture could be used, because the [MnCl(TPP)] could be washed off the silica support after **6** had been tethered to the support. In all three complexation reactions almost all TMS-protecting groups were cleaved during the reaction. Tetrabutylammonium fluoride (TBAF) was added to the reaction mixtures to ensure cleavage of all TMS groups, but in most instances was not necessary.

Ethynyl-functionalised porphyrin ligand **2** and metallo-porphyrins **3**, **4**, and **6** were reacted with azide-functionalised silica in the presence of a copper catalyst (2-[dimethylamino)methyl]-1-thiophenolato-copper(I)) at room temperature in MeCN for four days. With free-base porphyrin **2** (TMS groups cleaved using TBAF) several attempts to immobilise on silica using 'click' techniques were made. However, we were unsuccessful with both the aforementioned copper(I) thiolate complex and also $[Cu(MeCN)_4]PF_6$ as catalyst. We found that transmetallation occurs between the copper(I) catalysts and the porphyrin ligand, thus deactivating the copper catalyst which resulted in very low yields of immobilised porphyrin ligand **2**. This led us to synthesise the 'protected' porphyrin material **4**, because, contrary to the copper porphyrin complexes, zinc containing porphyrins are known to be relatively labile and can be applied in demetallation and transmetallation reactions. Material **4** was reacted with azide-functionalised silica yielding material **8**. We attempted to demetallate the zinc containing material **8** using trifluoro-acetic acid (TFA). Spectroscopic studies (UV–Vis) of the resulting material confirmed that the demetallation process to yield immobilised free-base porphyrin material **11** was successful. However, we found it very difficult to remove all the formed non-porphyrin zinc(II) salts from the silica material. The zinc elemental content only dropped from 0.24% to 0.14% even after carrying out several thorough washing techniques, and IR spectroscopy gives indications of acetates on the silica surface.

Materials **7**, **8**, and **9** were successfully synthesised (Scheme 3). Ethynylbenzene was subsequently added to the reaction mixture to ensure 'capping' of any remnant azide groups on the silica surface. In the case of materials **7** and **8** it was difficult to gather experimental proof that all ethynyl groups had reacted with surface azide groups. Therefore, extra free hexylazide was added to the reaction mixture to ensure any remnant ethynyl groups were 'capped' to ensure they did not influence any future applications of the materials. The obtained materials were either dark green in colour (manganese containing materials **7** and **9**) or light pink (zinc containing material **8**). Model system **10** was also synthesised for spectroscopic purposes, to monitor both the electronic effects of having triazole-substituents bound to the porphyrin backbone and to study the influence of the support material on the porphyrin metal complex itself.

It is important to note that test reactions were carried out to monitor if transmetallation between the copper(I) thiolate complex ('click' catalyst) and the porphyrin–manganese/zinc complexes had occurred during the immobilisation procedure. This was found not to be the case, demonstrating the effectiveness of using the copper catalysed coupling reaction for high yielding, clean, side-product-less immobilisation. No signs of transmetallation were observed (MALDI-ToF mass analysis) when a stoichiometric 1:1 molar mixture of copper(I) thiolate and metalloporphyrins **3**, **4**, or **6**, were mixed together under standard 'click' reaction conditions. No signals pointing to copper porphyrin formation were observed, and likewise no manganese or zinc thiolate signals were observed. Furthermore, it was found that neither complexes **3**, **4**, or **6** catalyse the 1,3-Huisgens dipolar cycloaddition reaction.

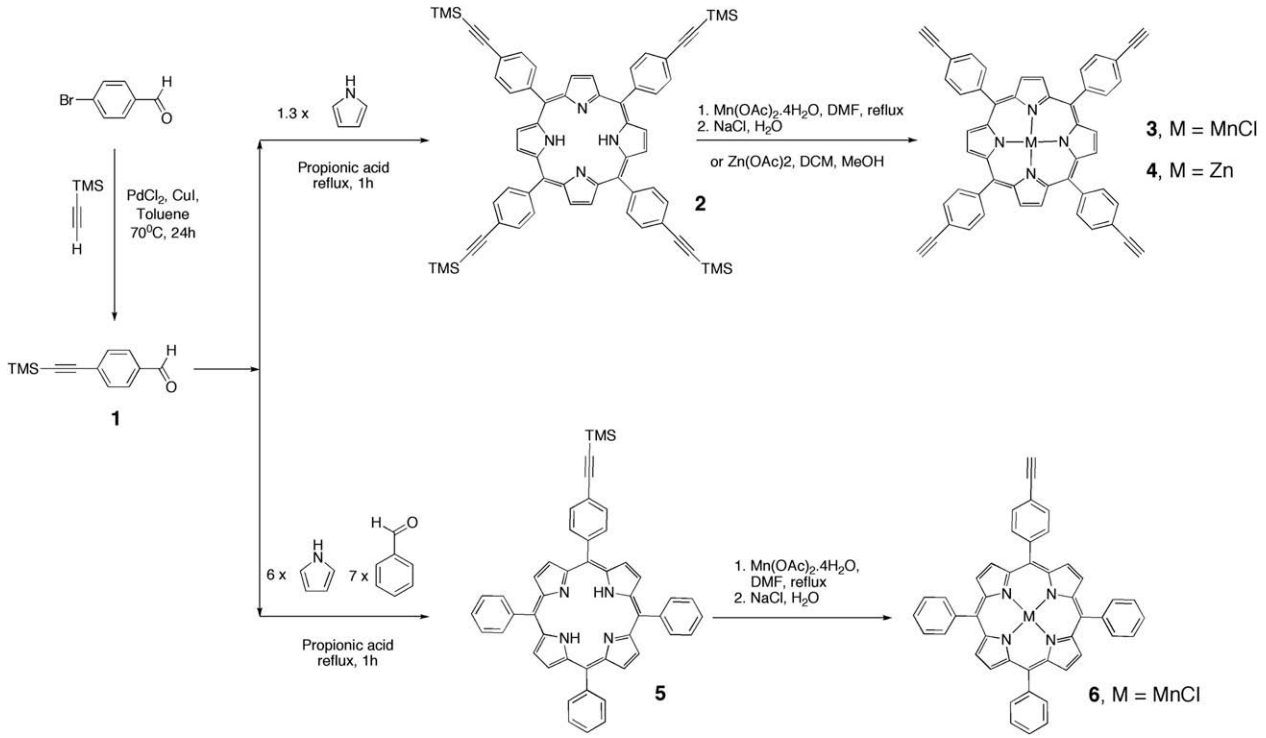

Scheme 2. Synthesis of mono- and tetra- functionalised porphyrin complexes for tethering to silica support material.

2.2. Elemental content analysis of Mn–porphyrin materials

The manganese loading of materials **7** and **9** was found to be approximately 0.1% per weight of the total silica mass (1.8×10^{-5} mol/g Mn on SiO_2). The nitrogen loading of materials **7**, **8**, and **9** is less than the azide-functionalised silica material (0.5–1.0% vs. 1.39% for starting azide material). However, the decrease in nitrogen loading is to be expected because the ethynyl–phenyl functionalised manganese porphyrin is a large macromolecule with a large carbon content, which would be expected to result in diminished relative nitrogen content measurement (even though it contains four nitrogen's itself). This is backed up by the relatively large carbon content (18% for material **7**). The relative nitrogen to manganese loadings would suggest that there are 20 nitrogen atoms for every manganese atom in material **7** – suggesting complete tethering of all four ethynyl groups to the silica surface (expected 16 N for every 1 Mn).

2.3. Surface area measurements

BET surface area measurements were used to analyse the starting azide material [11]. The starting azide material was chosen because it gives a reliable and general indication of the surface landscape relative to all materials presented herein. The surface area of the unfunctionalised silica starting material was approximately 218 m^2/g. The azide-functionalised material showed a surface area of 208 m^2/g. This is an expected decrease, which comes with the coupling of organic moieties to the silica surface, thus decreasing the surface area. The pore diameter and volume measurements also gave valuable information about catalyst site accessibility. We set out to immobilise catalysts without having influences from the support material. This is reflected in the observed pore volumes for the azide material vs. the starting silica material. On loading the silica material with the tethering functionality, the pore volume drops minimally. The observed large pore volumes (~1 cm^3/g) and the observed pore size (16–17 nm)

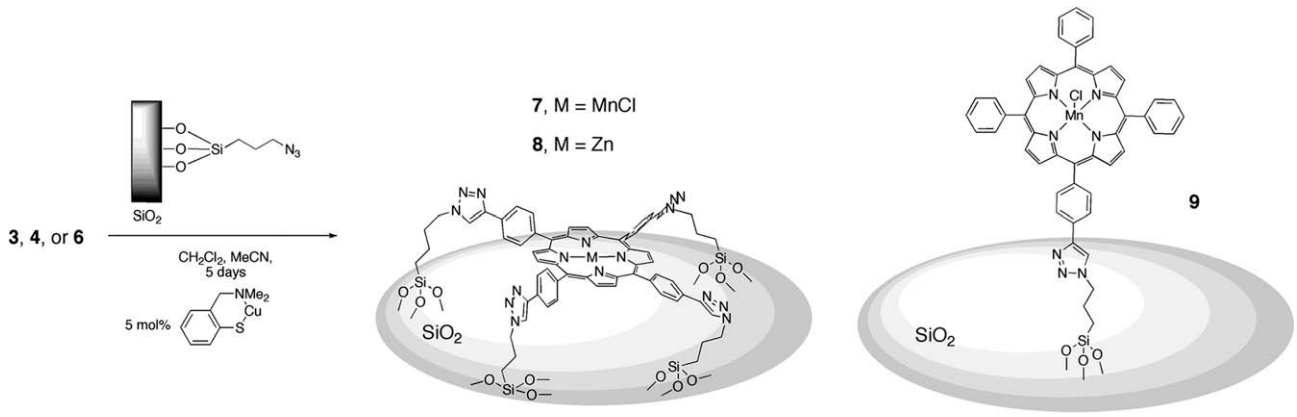

Scheme 3. Immobilisation of functionalised porphyrin complexes on silica support using copper(I) thiolate catalysed click chemistry.

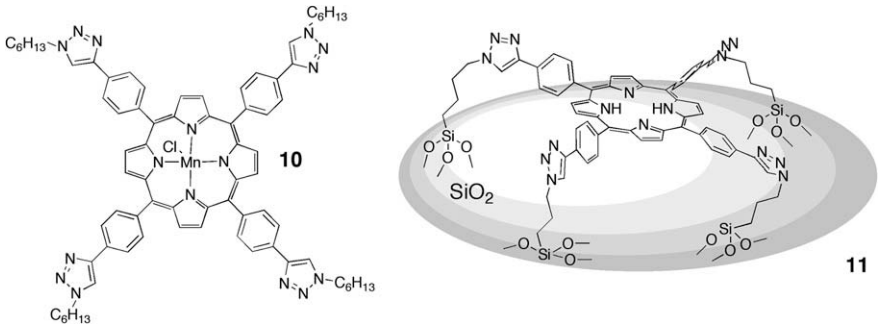

Fig. 1. Soluble model system for immobilised manganese complexes, **10**, and insoluble immobilised free-base porphyrin material **11**.

means it is highly unlikely that the support has much influence on the kinetics (mass transport) of the catalytic reactions (see Table 1).

By combining the nitrogen content analysis results of the azide material with the BET surface area results we can get an indication of the 'area' *per* a single catalytic site, and the proximity of catalytic sites to each other. This point is more relevant to material **9** (mono-dentate to silica surface) than **7** (multi-dentate to silica surface). This relies on the assumption that all azide sites are available for reaction with ethynyl-functionalised organometallic species, and the entire surface of the material is accessible to the organic moieties used to functionalise the material. The nitrogen content is 1.39% of the total loading, which gives 4.76×10^{-6} mol/m^2 nitrogen loading. This can be converted to functionality loading by dividing by three (three nitrogen's for every azide) which gives 1.59×10^{-6} mol/m^2 (1.59×10^{-26} mol/Å^2) azide loading. Using Avogadro's constant this gives an approximation that every azide group sits on 104.4 Å^2. Simplifying the calculations even further, we can estimate the 'ideal situation' distance between azide sites. Assuming that all azide sites are equally deposited on the silica surface, we treat every functionality site as a cylinder lying perpendicular to the silica surface. The estimated radius (r) of the area around a catalytic site could be acquired from πr^2 = area. Therefore, the average distance between catalytic sites is equal to $2r$, and thus is 11.3 Å. This distance is relatively small and has consequences for both materials **7** and **9**. The relatively short distance suggests that material **7** can readily bind to the silica surface with more than one of its ethynyl functionalities. Thus confirming the elemental analysis results which suggest the same from the Mn:N content. In material **9** the relatively short distance would allow for easy inter-catalytic site interactions which is discussed further later in this report.

2.4. UV–Vis analysis of Mn– and Zn–porphyrin materials

Solid-state diffuse-reflectance UV–Vis spectroscopy was used to analyse materials **7**, **8**, and **9**. The acquired spectra for **7** and **9** were compared to solution-state transmission spectra of compound **10** and [MnCl(TPP)] respectively (Fig. 2). The solid-state spectra confirm that metallo-porphyrin species have been immobilised on the silica surface, with minimal changes in the photophysical properties of the coordination complexes bound to the support. Material **7** shows a Soret band at 479 nm, which is comparable with both reference complexes **10** and [MnCl(TPP)]. Similarly, the Q-band region of the spectrum shows results comparable to those of the untethered complexes. Material **9** shows contrasting results to material **7** with a considerable blue shift in both the Soret band and the Q-bands compared to the reference compounds. The strong blue shifts observed upon immobilisation indicate aggregation of porphyrins by π-stacking on the silica surface [12]. This observation can tell us a lot about *both* materials **7** and **9**. It appears that with only one site for tethering of the porphyrin ring to the inorganic support (material **9**), high levels of inter-porphyrin interaction on the surface are possible (see surface area analysis results). Because no blue shift is observed in the spectrum of **7** we assume the multiple anchoring of the porphyrin prevents this stacking. This would suggest that inter-porphyrin interactions are highly likely when there is a single appendage between the porphyrin ring and the silica surface, because the porphyrin lies perpendicular to the silica surface, and is relatively mobile. In material **7**, because there are four possible appendages between the porphyrin ring and the silica surface, the porphyrin is probably forced to be parallel to the silica surface, and thus inter-porphyrin interactions are unlikely.

Material **8** was also characterised using solid-state UV–Vis spectroscopy and the subsequent demetallation of material **8** was monitored. Fig. 3 depicts the solid-state UV–Vis reflectance spectrum of material **8** and the solid-state spectrum of material **11**, which is formed after demetallation of material **8**. The latter material shows characteristic absorptions of free-base porphyrin species. The fact that positioning of the Soret band and the Q-bands have shifted considerably with respect to **8** is characteristic of an uncoordinated porphyrin ligand.

Table 1
BET surface area, pore volume and size measurements.

Material	Surface area (m^2/g)	Pore volume (cm^3/g)	Pore size (nm)
Starting **SiO$_2$**	218.40	1.13	20.61
Azido-**SiO$_2$**	208.20	0.92	17.62

2.5. Infra-red analysis of porphyrin materials

Porphyrin containing materials were also studied with ATR-IR [13] and DRIFT [14] techniques. Fig. 4 depicts the DRIFT difference spectra pertaining to material **7**. The results observed are indicative for all porphyrin bound materials synthesised (**7**–**11**). The DRIFT spectrum of the starting silica is subtracted from the spectrum of **7** giving an indication of what has been 'added' to the silica (Fig. 4a). The spectra show that a trough in the difference spectrum is observed at 3738 cm^{-1} which corresponds to a clear decrease in the intensity of silanol stretches demonstrating that all linker groups are covalently bound to the silica support. The decrease in silanol groups is a result of the synthesis of azide-functionalised material (Fig. 1). It demonstrates a covalent linkage between the silica support and the propyl-triazole linker is present. Fig. 4b confirms the reaction of ethynyl groups of the porphyrin complex with the azide group on the silica surface. The trough at 2037 cm^{-1} is the azide stretch of the starting material which has disappeared in material **7**. In both spectra a less intense resonance peak is ob-

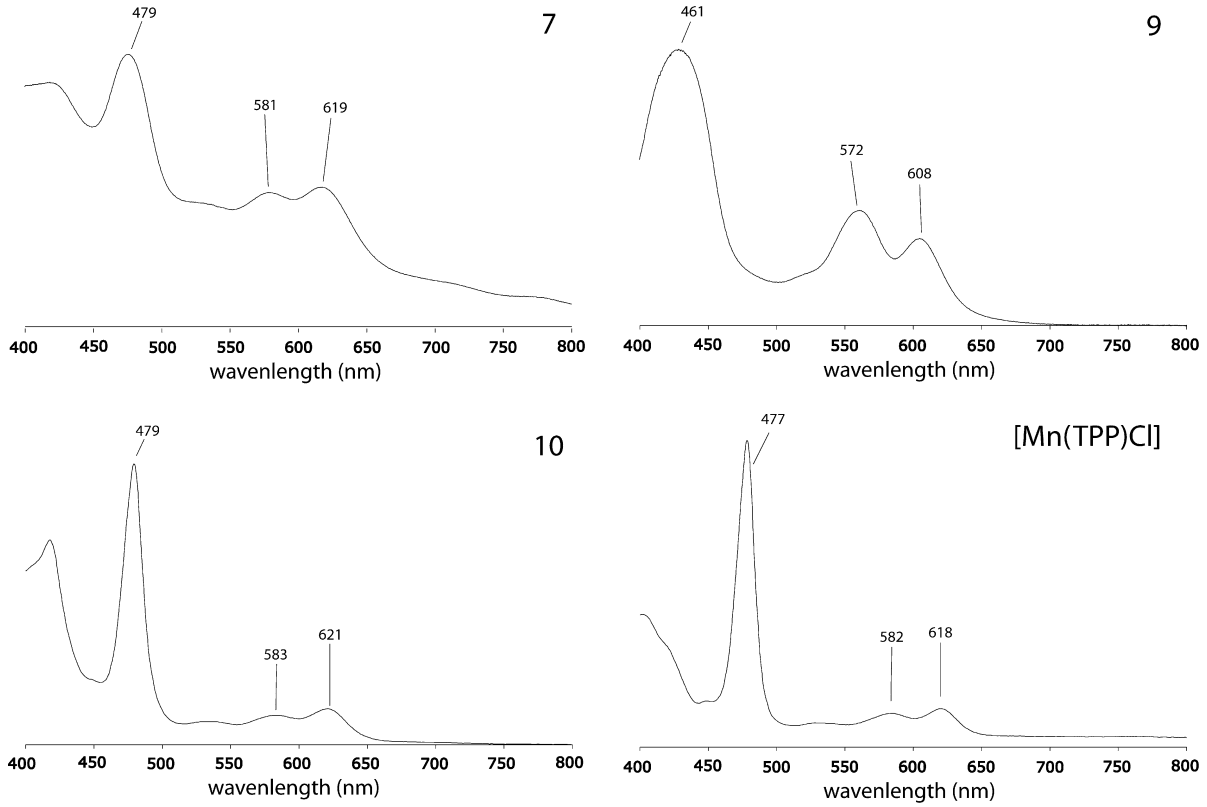

Fig. 2. Solid- and solution-state UV–Vis spectra of materials **7**, **9**, **10** and [MnCl(TPP)], respectively.

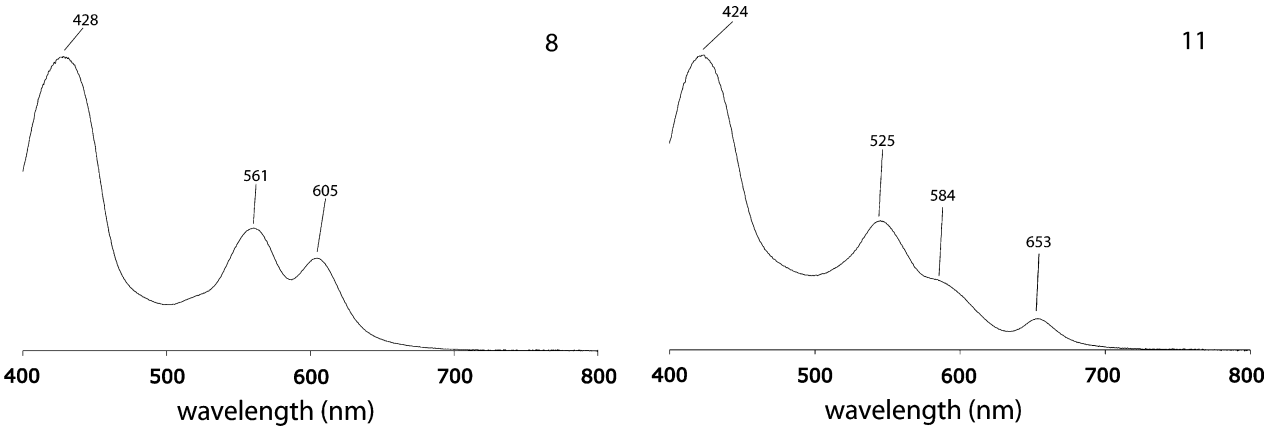

Fig. 3. UV–Vis solid-state reflectance spectra of materials **8** and **11**.

served at 1450 cm^{-1} which corresponds to the triazole groups of the 'clicked' final product (confirmed by ATR spectrum of **10**). These resonances are not observed in the starting material spectra. Due to the low amount of characteristic, intense IR resonances of metallo-porphyrin complexes, it was difficult to assign the remainder of the observed peaks. However, the broad resonances observed in the 3000–3500 cm^{-1} and 900–1300 cm^{-1} range are characteristic of the silica support material.

2.6. NMR analysis

^{29}Si CP-MAS NMR spectroscopy was applied to analyse the effects of carrying out organic synthetic techniques on the silica support. The ^{29}Si spectrum of organometallic containing material **7** showed several peaks that indicated the presence of different forms of silicon species at the surface and in the bulk of the material (Fig. 5). Peaks at −101 and −111 ppm are characteristic of Q type (Si-(O-)$_4$) silicates, which are in the bulk material. Peaks at −61 and −67 ppm are typical of T-type (R_1-Si-(O-)$_3$) silicates, that is, the silicon bound to the propyl group at the surface of the support. This is a clear indication that the catalyst is covalently bound to the support. The presence of double peaks in the −60 ppm (T^2 at 61 ppm, T^3 at 67 ppm) region indicates that not all ethoxy groups of functionalised propyl-1-triethoxysilane have reacted in the grafting process, and in some cases only two (thus nomenclature T^2) of the three have reacted. The single peak at 13 ppm is typical

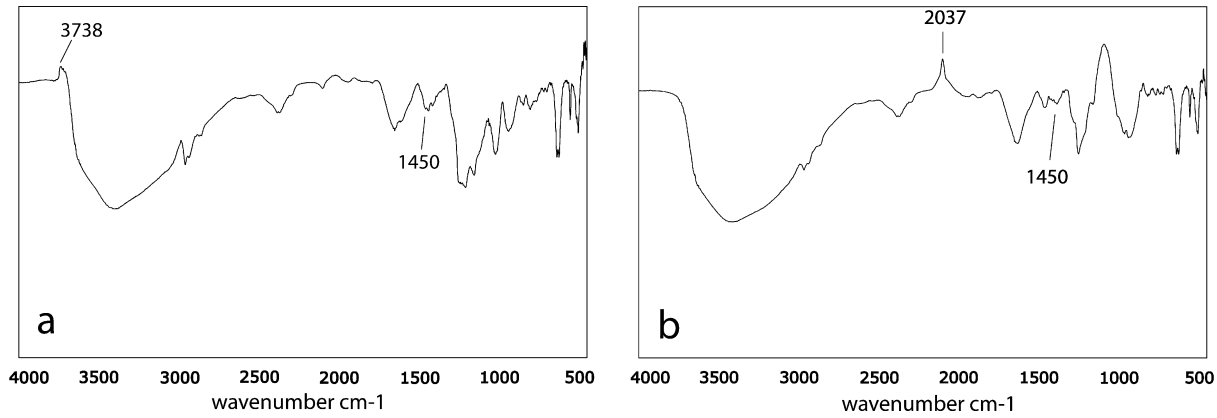

Fig. 4. IR DRIFT difference spectra of material **7**: (a) **7** minus SiO_2, (b) **7** minus azide-functionalised material.

of M-type (R_3-*Si*-(O-)) silicates (where R is the methyl groups of the trimethylsilyl capped silanol groups).

2.7. 'Heterogeneous' oxidation catalysis with Mn–porphyrin materials **7** and **9**

Materials **7** and **9** were applied as heterogenised catalysts in the epoxidation of various substrates. Various oxidants were used to monitor the effects of the oxidant properties on the stability and reusability of the heterogenised catalysts. Materials **7** and **9** were initially applied in the epoxidation of cyclooctene (COE) using iodosylbenzene (PhIO) as oxidant, and with imidazole introduced as a catalytic co-ligand (Table 2). Material **7** showed diminished activity compared to its homogeneous analogue, [MnCl(TPP)] (230 cf. 82 turnovers h^{-1}). The observed decrease in catalyst activity (on a per Mn site basis) is to be expected with the heterogenisation of homogeneous catalysts. However, the yield observed was 71% compared to 92% yield for the homogeneous system, which was unexpected (based on conversion of oxidant, alkene in excess). Material **9** showed low conversion levels and activity in the epoxidation of COE. This is surprising when compared to material **7**, however we believe it to be as a result of inter-porphyrin site interactions, resulting in intermolecular μ-oxo-bridged dimer formation (see following section). In fact the colour of the material **9** was quite brown compared to the dark green hue it had prior to catalysis. This would suggest MnO_2 formation. In all cases the kinetic profile of the catalysed epoxidation reaction is the same as the kinetic profile of the homogeneous catalyst, [MnCl(TPP)] (see Fig. 6).

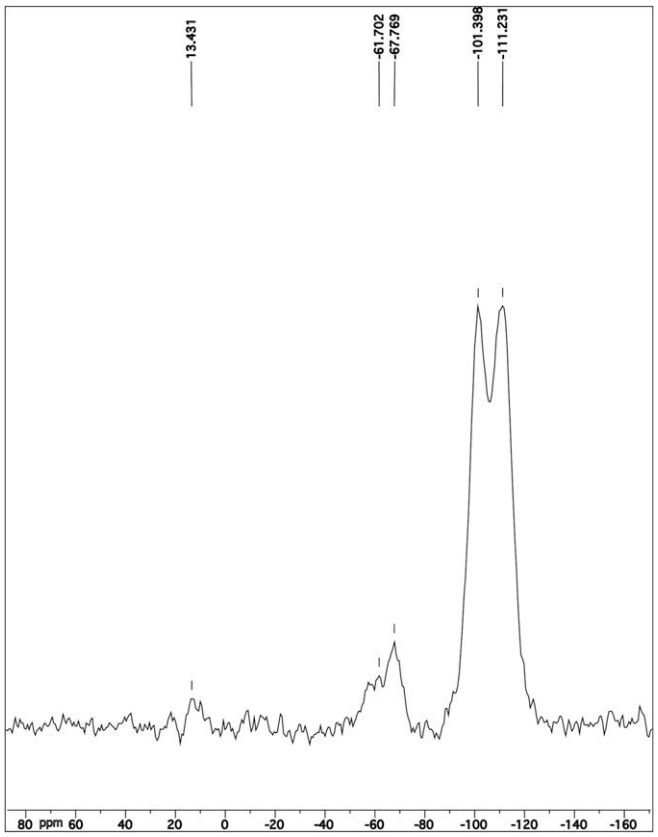

Fig. 5. Solid-state CP-MAS ^{29}Si NMR spectrum of material **7**.

Material **7** was applied as an epoxidation catalyst using other substrates to demonstrate the general applicability of these catalytic materials. Cyclohexene (CHE) and styrene (STE), which are less reactive substrates to manganese porphyrin catalysed epoxidation, were both tested using iodosylbenzene as oxidant. CHE was converted to cyclohexene epoxide (CHO) in very ordinary yields (~10%) with a TOF of 7.5 h^{-1}. Likewise STE was converted to styrene-epoxide (STO) in average yield (47%), however with a much higher TOF (58 h^{-1}) (see Table 3).

After the epoxidation of COE material **7** was recycled by simple filtration of the catalyst and subsequent washing of the solid remnants with CH_2Cl_2 and MeOH. A fresh solution of substrate, oxidant, and imidazole was then introduced to the catalytic material, and the catalysed reaction was restarted. In the epoxidation of COE catalyst recycling was carried out over four cycles. After every cycle the TOF decreased slightly and the yield decreased considerably, such that by the fourth cycle the TOF was under 20 h^{-1} and the yield was below 10% (Table 2). The post-catalysis filtrate was charged with extra alkene and oxidant, however showed no extra turnovers. This demonstrated that no Mn–porphyrin was leaching into the reaction solution. The observed gradual decrease in TOF and yields was a cause for concern, and thus we investigated the effects of other oxidants on the stability and durability

Table 2
Application of materials **7** and **9** in the epoxidation of COE.

Catalyst	Yield epoxide (%)[a]	TOF[b]
[MnCl(TPP)]	92	230
7	71	82
9	13	8.5

[a] Based on iodosylbenzene consumed.
[b] Based on rate of epoxide formation (h^{-1}).

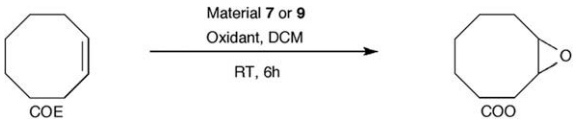

Fig. 6. Epoxidation of COE using catalytic materials **7** or **9**.

Table 3
Recycling of materials **7** in the epoxidation of cyclooctene

Cycle #[a]	PhIO TOF[b]	BPO TOF[c]
1	76	3.4
2	66	2.9
3	40	1.7
4	20	1.0
5	–	0.4

[a] Catalyst recycled by simple filtration and washing.
[b] Based on rate of iodosylbenzene consumption (h^{-1}).
[c] Based on rate of *t*-butylperoxide consumption (h^{-1}).

of the catalytic material **7**. The milder oxidising agent *t*-butylperoxide (BPO) was applied in the epoxidation of COE using material **7** as a catalyst. The initial reaction using BPO showed considerably lower conversion levels and TOF's compared to PhIO (Table 2). This is to be expected and is due to the better oxidising powers of PhIO compared to BPO. Material **7** was recycled in the same manner and fresh substrate and BPO were added to the separated catalytic material. However, a similar deactivation trend was observed. Material **9** was not recycled because of the poor catalytic ability of the material, and furthermore the visible decomposition of the manganese–porphyrin complex on the silica surface.

The properties of material **7** after application as a catalyst in the epoxidation of COE were investigated to gain insights into the deactivation pathways. The elemental content of the post-catalysis material showed that the Mn loading had not changed at all, even after five catalyst cycles (0.1% Mn before catalysis, 0.1% after catalysis). Solid-state UV–Vis and DRIFT-IR spectroscopy were used to analyse the material as well (Fig. 7). In particular, the UV–Vis spectrum is comparable to that of material **7** and [MnCl(TPP)], however this result must be tempered by the fact that the spectrum is very broad, which thus limits the accuracy. Both spectra suggest that the integrity of the manganese–porphyrin complex has been retained and the integrity of the silica support has been maintained – no extra silanol resonance were observed in the IR spectrum. The DRIFT-IR difference spectrum show that nothing new has been added to the silica surface, and that the triazole species remains intact.

2.8. Catalysts deactivation discussion

Supported Mn-complex deactivation is a very common occurrence in epoxidation catalysis. Several reports have commented on Mn–salen systems bound to supports which show gradual deactivation upon recycling of the catalytic materials [15]. In these systems, the deactivation was believed to be as a result of decomplexation of the Mn–salen complexes bound to the silica support. Likewise Mn–porphyrins supported on polymeric supports have shown deactivation upon recycling in epoxidation catalysis.[16] In some cases the deactivation is put down to bleaching of the manganese–porphyrin complexes by intermolecular oxidation, resulting in decomplexation. The precursor to the decomplexation is a μ-oxo-bridged dimer which is also inactive in epoxidation catalysis. In most cases a convincing reason for deactivation is *not* given.

In the case of material **7**, we do not believe that any intermolecular interactions between porphyrin complexes on the silica surface are occurring. Firstly no UV–Vis evidence for this was observed, and secondly, the multi-dentate manner in which the complex is bound to the surface probably means the porphyrin ring lies in such a position that inter-porphyrin site interactions are unlikely. Obviously this does not tell us about all porphyrin sites on the silica surface, but gives an indication that most have retained their structural integrity. However, the solid-state UV–Vis technique employed is quite crude. In previous reports accumulation of by-products was believed to deactivate the catalyst. PhIO reacts with itself giving iodobenzene (PhI) and iodoxybenzene ($PhIO_2$). It is believed that $PhIO_2$, having low solubility in the reaction solvent, accumulates on the support surface and blocks access to the active site [17]. However, here, post-catalytic elemental analysis shows no iodine content, thus proving conclusively that iodoxybenzene plays no role in the deactivation of the catalytic material. Activation of the active site by imidazole coordinating to the manganese centre is possibly inhibited by the manner by which the complex is bound to the silica support. The incoming imidazole binds either on the face of the porphyrin which points away or towards the silica surface and thus activates the opposite axial site for oxidation. It is possible that if the imidazole binds the face pointing away from the silica surface, that the active site may be prone to interactions with the silica surface or functional groups on the silica surface. Oxidation of these functional groups would likely create a hydroxyl moiety which could bind the Mn site, or if not bind, block access to the active site. However, we presently have no concrete evidence for this hypothesis. Finally, magnetic stir bars are used to stir the catalytic solution. This often leads to pulverisation of the catalytic material, and possibly mechanical decomposition of the silica material. As all spectroscopic

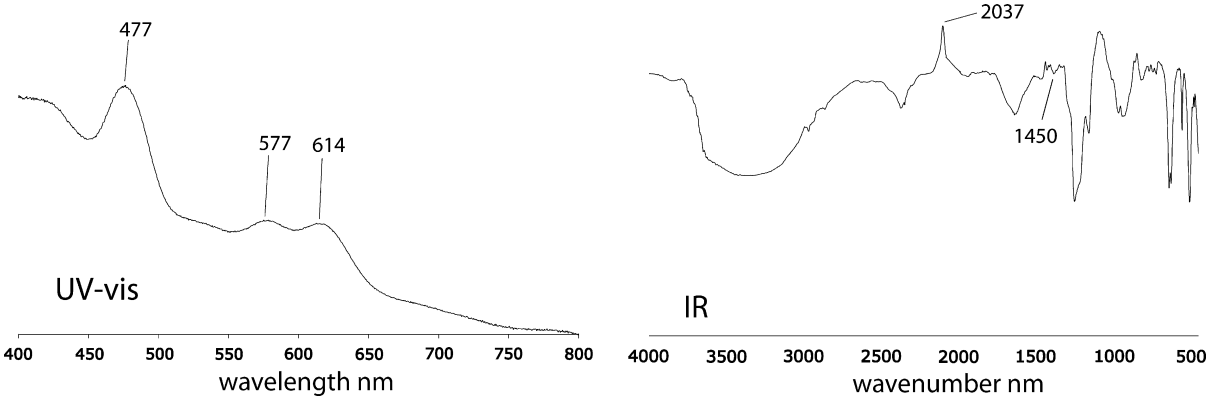

Fig. 7. Post-catalysis solid-state UV–Vis and IR spectra of material **7**.

techniques indicate that both the manganese complex, and silica support remain sound during catalysis, we propose that a combination of the above-mentioned decomposition pathways is the reason for gradual catalyst deactivation over five cycles.

In the case of material **9** we did not attempt recycling experiments because of the poor results observed. Material **9** gives maximum epoxide yields of 13%, and shows no catalytic turnovers upon the addition of fresh substrate. We believe the deactivation to be as a result of inter-porphyrin interactions that are resulting in active site blockage and eventual decomplexation.

3. Conclusions

Metallo-porphyrins have been immobilised on silica using 'click' techniques. The 'click' immobilisation procedure is highly efficient, and demonstrates a simple lab shelf to reaction vessel procedure for the application of heterogenised homogeneous catalysts. No side products are formed in the immobilisation procedure, no activating reagents are required, and there are no traces of the copper catalyst used in the coupling reaction. This click immobilisation alleviates the necessity for extreme reaction conditions, or even the use of base or acid to allow coupling between complex and support. The developed materials contain complexes bound to silica in both a monodentate and polydentate manner, and a notable difference is observed between the two. Monodentate appendage to the support allows freedom of movement of the porphyrin complexes, resulting in inter-porphyrin interactions, and deactivation. Polydentate immobilisation of porphyrin complexes yields active catalytic materials. The catalytic materials become deactivated over a number of catalyst recycles, and this is as a result of side-product accumulation on the silica surface. The polydentate immobilisation may enhance the deactivation of the immobilised catalysts because the active site may be trapped between the silica surface and the porphyrin ring system.

4. Experimental

4.1. General considerations

Standard Schlenk procedures under N_2 were carried out throughout. Reagents were used as supplied from Acros BV or Sigma–Aldrich, unless otherwise stated. ^{1}H, ^{13}C and ^{31}P solution NMR was carried out on a Varian Inova 300 spectrometer or a Varian Oxford AS400. CP-MAS NMR was carried out using a Bruker AV 750. Elemental analyses were performed by Dornis und Kölbe, Mikroanalytisches Laboratorium, Mülheim a. d. Ruhr, Germany. MS measurements were carried out on an Applied Biosystems Voyager DE-STR MALDI-TOF MS. IR spectra were recorded on a Perkin–Elmer SpectrumOne FT-IR Spectrometer. GC analyses were performed on a Perkin-Elmer AutosystemXL Gas Chromatograph. Solution UV–Vis spectra were recorded on a Varian Cay 50 Scan UV–Vis spectrophotometer and diffuse-reflectance UV–Vis spectra were recorded on a Cary 5 UV–Vis – NIR spectrophotometer.

4.2. 5,10,15,20-Tetrakis-(4-[(trimethylsilyl)ethynyl]phenyl)porphyrin (**2**)

A solution of 4-[(trimethylsilyl)ethynyl]-benzaldehyde (8.0 g, 39.5 mmol) in propionic acid (ca. 180 mL) was brought to reflux temperature. Pyrrole (3.2 mL, 49 mmol) was added and the mixture turned immediately black. The mixture was stirred at reflux for 1 h after which it was allowed to cool to room temperature. A black solid precipitated and the suspension was allowed to settle overnight. The black liquid was removed by filtration and the remaining black solid was washed with methanol until the filtrate was colourless. The remaining purple solid was recrystallised from CH_2Cl_2 and MeOH (yield: 4.7–8.2%). ^{1}H NMR ($CDCl_3$, ppm): δ −2.84 (NH, s, 2H), 0.372 (Si-CH_3, s, 36H), 7.86 (*m*-ArH, d, ^3J = 7.80 Hz, 8H); 8.14 (*o*-ArH, d, ^3J = 7.80 Hz, 8H); 8.81 (β-H, s, 8H). ^{13}C NMR ($CDCl_3$, ppm): 0.253 (Si-CH_3); 40 ($(CH_3)_3$Si-C≡C); 51 ($(CH_3)_3$Si-C≡*C*); 120 (C_{meso}); 127 ($ArC_{3,5}$); 128 (ArC_4); 131 (C_β); 135 ($ArC_{2,6}$); 139 (ArC_1); 142 (C_α); UV–Vis (CH_2Cl_2): $\lambda_{max/nm}$ (log ε): 422 (5.78); 517 (4.38); 553 (4.17); 592 (3.87); 648 (3.87). MALDI-TOF (*m*/*z*): 1000.02 (calc. 999.55).

4.3. 5,10,15,20-Tetrakis-(4-(ethynyl-phenyl)porphyrinmanganese(III) chloride (**3**)

To a purple solution of 5,10,15,20-tetrakis-(4-[(trimethylsilyl)ethynyl]phenyl)porphyrin (50 mg 0.05 mmol) in DMF (ca. 30 mL), $Mn(OAc)_2 \cdot 4H_2O$ (250 mg, 1 mmol) was added and the mixture was stirred at reflux temperature overnight, during which it turned dark green. The solution was allowed to cool to room temperature. It was added to an ice cooled NaCl-solution (10 g/40 mL) and a precipitate a dark green precipitate formed that was recovered by filtration. The green solid was dissolved in dichloromethane and saturated NaCl-solution was added. After stirring at room temperature for 3 h the organic layer was separated dried over $MgSO_4$. Cleavage of the TMS groups was checked using MALDI-TOF. If the cleavage was not complete, an extra reaction step was performed in which the dichloromethane was removed in vacuo and the remaining green solid was dissolved in THF (ca. 10 mL). A solution of tetra-butylammonium fluoride (TBAF) in THF (1 M, 0.5 mL, 0.5 mmol) was added. The reaction was quenched by the addition of water and a precipitate formed. The liquid was removed by filtration after which the green solid was dissolved in dichloromethane and dried over $MgSO_4$. The green solution was concentrated in vacuo before it was loaded on a column containing dry, neutral alumina. After elution with 5% MeOH in $CHCl_3$ a small purple fraction was collected, followed by a green product fraction. The solvent was removed in vacuo, yielding 44% of a dark green solid. UV–Vis (CH_2Cl_2): $\lambda_{max/nm}$ (log ε): 376 (4.44); 403 (439); 421 (4.39); 478 (4.72); 526 (3.52); 585 (3.68); 619 (3.75). MALDI-TOF (*m*/*z*): 763.75 (calc. 799.20; without Cl 763.75).

4.4. 5,10,15,20-Tetrakis-(1-hexyl-4-phenyl-1,2,3-triazolo)porphyrinmanganese(III) chloride (**10**)

To a solution of *5,10,15,20-tetrakis-(4-(ethynyl-phenyl)porphyrinmanganese(III) chloride* (50 mg, 0.075 mmol) in dry and degassed CH_3CN was added hexylazide (65 μL, 0.45 mmol), followed by addition of 2,6-lutidine (8.5 μL, 0.075 mmol) and a spatula tip of $[Cu(MeCN)_4]PF_6$. The mixture was stirred at room temperature for 3 days, after which the CH_3CN was removed in vacuo. The remaining green oil was dissolved in dichloromethane and washed with water (2×). After drying over $MgSO_4$ the dichloromethane was removed in vacuo, yielding a green oily solid 30%. UV–Vis (CH_2Cl_2): $\lambda_{max/nm}$ (log ε): 381 (5.32); 418 (5.40); 479 (5.56); 528 (3.59); 583 (3.65); 621 (3.72). MALDI-TOF (*m*/*z*): 1272.35 (calc. 1307.95, –Cl 1272.50).

4.5. 5,10,15,20-Tetrakis-(4-[(trimethylsilyl)ethynyl]phenyl)porphyrinzinc(II)

5,10,15,20-tetrakis-(4-[(trimethylsilyl)ethynyl]phenyl)porphyrin (63 mg, 0.08 mmol) was dissolved in CH_2Cl_2 (ca. 50 mL) and a solution of $Zn(OAc)_2 \cdot 2H_2O$ (365 mg, 1.66 mmol, 20 eq,) in MeOH (ca. 5 mL) was added. After 2 h stirring at room temperature, the solvent was removed in vacuo and the remaining purple-pink solid was dissolved in CH_2Cl_2 (5 mL) and eluted through a silica column

with CH_2Cl_2 as eluent. A pink fraction was collected. The pink solution was concentrated in vacuo and recrystallised from CH_2Cl_2/hexanes (yield: 34.4%). ^{1}H NMR ($CDCl_3$, ppm): δ 0.378 (Si-C*H*$_3$, s, 36H), 7.88 (*m*-ArH, d, ^3J = 7.50 Hz, 8H); 8.16 (*o*-ArH, d, ^3J = 7.20 Hz, 8H); 8.93 (β-H, s, 8H). UV–Vis (CH_2Cl_2): $\lambda_{max/nm}$: 423; 550; 589.

4.6. 5,10,15,20-Tetrakis-(4-(ethynyl)phenyl)porphyrin-zinc(II) (**4**)

TBAF (1 M in THF, 120 μL, 0.12 mmol) was added to a solution of (5,10,15,20-tetrakis-(4-ethynylphenyl)porphyrin-Zn(II) (29.3 mg, 0.03 mmol) in dry THF (ca. 20 mL). After stirring at room temperature for 30 min, the reaction was quenched with water and a pink solid precipitated. The solvent was removed by filtration, yielding a pink solid (yield: 95%). ^{1}H NMR (DMSO, ppm): δ 4.46 (acetyleneH. s, 4 H); 7.92 (*m*-ArH, d, ^3J = 7.80 Hz, 8H); 8.20 (*o*-ArH, d, ^3J = 8.10 Hz, 8H); 8.81 (β-H, s, 8H). UV–Vis (CH_2Cl_2): $\lambda_{max/nm}$ (log ε): 422 (5.74); 548 (4.35); 587 (3.70). MALDI-TOF (*m*/*z*): 772.41 (calc. 772.16).

4.7. 5-(4-[(Trimethylsilyl)ethynyl]phenyl)-10,15,20-trisphenylporphyrin (**5**)

A solution containing 4-[(trimethylsilyl)ethynyl]-benzaldehyde (296 mg, 1.34 mmol, 1 equiv.) and benzaldehyde (0.8 mL, 7.8 mmol, 5.8 equiv.) in propionic acid (ca. 40 mL) was brought to reflux temperature. Pyrrole (0.7 mL, 9.1 mmol, 6.8 equiv.) was added and the mixture turned immediately black. The mixture was stirred for 1 h after which it was allowed to cool to room temperature. A black solid precipitated and the suspension was allowed to settle overnight. The black liquid was removed by filtration and the remaining black solid was washed with methanol until the filtrate was colourless. The crude product was used in further reaction steps.

4.8. (5-(4-[(Trimethylsilyl)ethynyl]phenyl)-10,15,20-trisphenylporphyrin)manganese(III)chloride (**6**)

The remaining solid (from porphyrin synthesis reaction) was dissolved in DMF (ca. 40 mL) and $Mn(OAc)_2 \cdot 4\ H_2O$ (250 mg, 1 mmol) was added. The mixture was refluxed overnight. The formed green solution was allowed to cool to room temperature. It was added to an ice cooled NaCl-solution (10 g/40 mL) and a precipitate was formed that was removed by filtration. The green solid was dissolved in CH_2Cl_2 and saturated NaCl-solution was added. After stirring at room temperature for 3 h the organic layer was separated dried with $MgSO_4$. The green solution was concentrated in vacuo before it was loaded on a silica column prepared with a mixture of hexanes and CH_2Cl_2 (3:1 v/v). First, a purple fraction was eluted followed by a small green fraction. Methanol (5%) was added to the eluent and a green product fraction was eluted, followed by a dark green band. The presence, in one of the fractions, (5-(*p*-acetylenephenyl)-10,15,20-triphenylporphyrin)Mn(III)Cl was confirmed by MALDI-TOF. However, the same fraction also contained [Mn(III)(TPP)Cl]. This could not be separated from the other compound. The liquid was removed and the green solid was dried in vacuo. The mixture of functionalised and unfunctionalised porphyrin was used in the immobilisation process. MALDI-TOF (*m*/*z*): 667.70 ([MnCl(TPP)]), 691.36 (calc. 727.13; without Cl 691.68).

4.9. Procedure for porphyrin immobilisation

A porphyrin bearing free acetylene groups (50 mg) was dissolved in dry, degassed CH_3CN (10 mL). TMS-capped-3-azidopropyl-1-silica (500 mg) was added, together with a spatula tip of 2-[dimethylamino)methyl]-1-thiophenolato-copper(I) catalyst. After 5 days stirring under N_2 at room temperature, the solvent was removed by filtration and the green solid was washed with CH_2Cl_2 (2×), water and hot MeOH (2×) and dried in vacuo. The immobilised porphyrin was then again suspended in dry toluene and degassed for 15 min ethynylbenzene (0.5 mL) was added as well as a spatula tip of copper(I) aminoarenethiolate catalyst and the mixture was stirred for 3 days under N_2 at room temperature. The liquid was removed by filtration, followed by washing with CH_2Cl_2 (2×), hot MeOH (2×) and water. The remaining solid was dried in vacuo. The solid was once again suspended in toluene and degassed for 15 min. Hexylazide (1 mL) was added together with a small amount of copper(I) aminoarenethiolate catalyst and the mixture was stirred for 3 days under N_2 at room temperature. The liquid was removed by filtration and the solid was washed with CH_2Cl_2 (2×), hot MeOH (2×) and hexanes. Drying in vacuo yielded the final product. The loadings of the different catalysts were quantified by elemental analysis.

4.9.1. Material **7**

^{29}Si MAS CP (ppm): δ −111 (Q^4 silica); −101 (Q^3 silica); −61 (T^2, T^3 $RSi(O\text{-})_3$); 16 ($\text{-}CH_2SiO\text{-}$). UV-VIS: $\lambda_{max/nm}$: 479; 526 (sh); 581; 619. IR (DRIFT, difference, cm^{-1}): ν_{CH} 2967; $\nu_{triazole}$ 1460–1440. Elemental analysis found: C, 18.03; H, 0.95; N, 0.50; Mn, 0.10%.

4.9.2. Material **8**

UV–Vis: $\lambda_{max/nm}$: 428; 561; 605. IR (DRIFT, difference, cm^{-1}): ν_{CH} 2961; $\nu_{triazole}$ 1460–1440. Elemental analysis found: C, 9.49; H, 2.06; N, 0.96; Zn, 0.24%.

4.9.3. Demetallation of **8**, material **11**

TFA (30 μL, 0.42 mmol) was added to a suspension of X in CH_2Cl_2 (ca. 5 mL) upon which the mixture turned green immediately. After stirring for 1 h at room temperature the mixture was poured in saturated $NaHCO_3$ (50 mL) solution. The mixture turned pink again upon stirring and a pink solid precipitated. The liquid was removed by filtration and the solid was dried in vacuo. UV–Vis: $\lambda_{max/nm}$: 424; 545; 584 (sh); 653. IR (DRIFT, difference, cm^{-1}): ν_{NH} 3449; ν_{CH} 2951. Elemental analysis found: C, 10.50; H, 2.62; N, 0.61; Zn, 0.14%.

4.9.4. Material **9**

UV–Vis (CH_2Cl_2): $\lambda_{max/nm}$: 461; 529; 572; 608. IR (DRIFT, difference, cm^{-1}): ν_{arCH} 3057; ν_{CH} 2964; $\nu_{triazole}$ 1440–1420. Elemental analysis found: C, 17.71; H, 1.59; N, 0.69; Mn, 0.05%.

4.10. Standard alkene epoxidation catalysis conditions

Cyclooctene, cyclohexene and styrene were distilled prior to use. Cyclooctene and cyclohexene were filtered over neutral alumina prior to every catalytic reaction to remove trace amounts of epoxide. Iodosylbenzene was synthesised according to the literature procedure and *t*-butylperoxide was used as solution in decane. **Iodosylbenzene**: all experiments were performed at room temperature in small GC-vessels with magnetic stirring. All reagents were added as solutions in CH_2Cl_2, except iodosylbenzene and the supported catalysts. Catalyst (0.25 μmol active species) was stirred with the desired substrate (0.5 mmol), imidazole (5 μmol) and iodosylbenzene (0.03 mmol) in CH_2Cl_2. Product formation was monitored by taking small aliquots for GC analysis with 1,2-dibromobenzene as internal standard. ***t*-Butylperoxide:** all experiments were performed at room temperature in small GC-vessels with magnetic stirring. All reagents were added as solutions in MeCN except the supported catalysts. Substrate (0.3 mmol), catalyst (1 μmol), imidazole (0.02 mmol) and *t*-butylperoxide (0.02 mmol) were stirred in dichloromethane (2 mL). Product formation was

checked by taking small aliquots for GC analysis with phenyl bromide as internal standard.

4.11. Catalyst recycling

After each oxidation step, the reaction solution was removed by simple filtration and the catalytic material (solid) was washed with methanol. Fresh reagents were added and a subsequent catalytic experiment was performed.

Acknowledgement

The Dutch Technology Foundation (STW, DPC-5772) are kindly acknowledged for financial support.

References

[1] B. Cornils, W.A. Herrmann, J. Catal. 216 (2003) 23–31.
[2] D.E. De Vos, I.F.J. Vankelecom, P.A. Jacobs (Eds.), Chiral Catalyst Immobilization and Recycling, Wiley-VCH, Weinheim, 2000.
[3] H.-U. Blaser, Chem. Commun. (2003) 293–296.
[4] C. Baleizao, H. Garcia, Chem. Rev. 106 (2006) 3987–4043.
[5] E. Brule, Y.R. de Miguel, Org. Biomol. Chem. 4 (2006) 599–609.
[6] (a) P. Battioni, J.-P. Lallier, L. Barloy, D. Mansuy, Chem. Commun. (1989) 1149–1151;
(b) J.R. Lindsay Smith, Y. Iamamoto, F.S. Vinhado, J. Mol. Catal. A: Chem. 252 (2006) 23–30.
[7] A.R. McDonald, H.P. Dijkstra, B.M.J.M. Suijkerbuijk, M. Lutz, A.L. Spek, G.P.M. van Klink, G. van Koten, submitted for publication.
[8] H.C. Kolb, M.G. Finn, K.B. Sharpless, Angew. Chem., Int. Ed. 40 (2001) 2004–2021.
[9] A.D. Adler, F.R. Longo, J.D. Finarelli, J. Goldmacher, J. Assour, L. Korsakoff, J. Org. Chem. 32 (1967) 476.
[10] J. Rochford, D. Chu, A. Hagfeldt, E. Galoppini, J. Am. Chem. Soc. 129 (2007) 4655–4665.
[11] S. Brunauer, P.H. Emmett, E.J. Teller, J. Am. Chem. Soc. 60 (1938) 309–319.
[12] F. Odobel, E. Blart, M. Lagrée, M. Villieras, H. Boujtita, N. El Mur, S. Caramori, C.A. Bignozzi, J. Mater. Chem. 13 (2003) 502.
[13] ATR-IR (attenuated total reflection) is a technique whereby transmission of an IR beam through a sample is measured.
[14] DRIFT-IR (diffuse reflectance Fourier transform) is a surface technique which analyses reflected IR beam from the surface/near surface of the material.
[15] (a) M.D. Angelino, P.E. Laibinis, Macromolecules 31 (1998) 7581–7587;
(b) T.S. Reger, K.D. Janda, J. Am. Chem. Soc. 122 (2000) 6929–6934.
[16] (a) P.R. Cooke, J.R. Lindsay Smith, J. Chem. Soc., Perkin Trans. 1 (1994) 1913–1923;
(b) F.G. Doro, J.R. Lindsay Smith, A.G. Ferreira, M.D. Assis, J. Mol. Catal. A: Chem. 164 (2000) 97–108.
[17] (a) S. Camperstrini, B. Meunier, Inorg. Chem. 31 (1992) 1999;
(b) H.C. Sacco, Y. Iamamoto, J.R. Lindsay Smith, J. Chem. Soc., Perkin Trans. 2 (2001) 181–190;
(c) M. Bonnet, L. Schmid, A. Baiker, F. Diederich, Adv. Funct. Mater. 12 (2002) 39–42.